Aerosol and Air Quality Research, 20: 2780–2792, 2020
ISSN: 1680-8584 print / 2071-1409 online
Publisher: Taiwan Association for Aerosol Research
https://doi.org/10.4209/aaqr.2020.05.0195

Particulate Matter Concentrations in a Middle Eastern City – An Insight to Sand and Dust Storm Episodes

Tareq Hussein[1,2*], Xinyang Li[2], Qusay Al-Dulaimi[2], Shatha Daour[1], Nahid Atashi[2,3], Mar Viana[4], Andres Alastuey[4], Larisa Sogacheva[5], Sharif Arar[6], Afnan Al-Hunaiti[6], Tuukka Petäjä[2]

[1] *Department of Physics, The University of Jordan, Amman 11942, Jordan*
[2] *Institute for Atmospheric and Earth System Research (INAR), University of Helsinki, Helsinki FI-00014, Finland*
[3] *Faculty of Geographical science and Planning, University of Isfahan, Isfahan 8174673441, Iran*
[4] *Institute of Environmental Assessment and Water Research (IDAEA-CSIC), Barcelona 08034, Spain*
[5] *Climate Change Programme, Finnish Meteorological Institute, Helsinki, Finland*
[6] *Department of Chemistry, The University of Jordan, Amman 11942, Jordan*

ABSTRACT

In this study, the particulate matter mass (PM_{10} and $PM_{2.5}$) concentrations we measured during May 2018–March 2019 in an urban atmosphere of Amman, Jordan. The results showed that the annual mean PM_{10} concentration was 64 ± 39 µg m^{-3} and the $PM_{2.5}/PM_{10}$ ratio was 0.8 ± 0.2. According to the Jordanian Air Quality standards (JS-1140/2006), the observed PM_{10} annual mean value was below the limit value but that of the $PM_{2.5}$ was three times higher than the corresponding limit value. However, both exceeded the World Health Organization (WHO) air quality guideline values. In a larger perspective, the annual mean PM_{10} concentrations in Jordan were lower than what was reported in other cities in the Middle East but were higher when compared to other Mediterranean cities. During the measurement period, Jordan was affected by Sand and Dust Storm (SDS) episodes on 14 days. The source origins of these dust outbreaks were traced back to North Africa, the Arabian Peninsula, and the Levant. The 24-hour PM_{10} concentrations during these SDS episodes ranged between 108 and 188 µg m^{-3}, which was about 3–6 times higher than the mean values during clean conditions (~33 µg m^{-3}).

Keywords: Urban air quality; Particulate matter; Dust particles; Back-trajectory.

INTRODUCTION

Aerosols affect the Earth's atmosphere directly, e.g., by the scattering of solar radiation, which results in the cooling of the Earth's surface, and indirectly, e.g., by participating in cloud formation. In urban areas, aerosols originate from a vast range of local sources (natural and anthropogenic) and long-range transport. Aerosols have adverse health effects (Pope and Dockery 2006). Cardiorespiratory and lung problems have been often associated with long-term exposure and inhalation of dust particles (Pope *et al.*, 2002; Hoek *et al.*, 2013).

In general, a sand and dust storm (SDS) is by definition an aeolian processes that occur wherever there is a supply of granular material (typically inorganic grains with diameter smaller than 70 µm) and atmospheric wind of sufficient strength to move the grains (Kok *et al.*, 2012; Middleton, 2017). SDS episodes occur via three modes: saltation, when loose materials are removed from the surface and carried by the fluid, before being transported back to the surface, creep, and suspension (Gillette *et al.*, 1974; Shao *et al.*, 1993). During SDS episodes, dust particles are susceptible to turbulent fluctuations and can remain airborne for a short-term (diameter 20–70 µm) or long-term (diameter < 20 µm) (Natsagdorj *et al.*, 2003; Thomas *et al.*, 2005; Evan *et al.*, 2011; Kok *et al.*, 2012). Short-term suspended dust has a local effect whereas Long-term suspended dust stay airborne up to several weeks and be transported for thousands of kilometers from their source region (Gillette and Walker, 1977; Zender *et al.*, 2003; Miller *et al.*, 2006; Kok *et al.*, 2012; Zoljoodi *et al.*, 2013; Doronzo *et al.*, 2015; Gherboudj *et al.*, 2017).

The arid and semi-arid regions that have a supply of granular material are found in deserts, beaches, and etc. Airborne dust particles can be transported from their source area across thousands of kilometers affecting weather and climate, air quality, ecosystem productivity, hydrological

* Corresponding author.
Tel.: +358 2941 50709
E-mail address: tareq.hussein@helsinki.fi

cycle, and many components of the Earth system in addition to severe human health effects (Small *et al.*, 2001; Menendez *et al.*, 2007; McTainsh and Strong, 2007; Goudie, 2009; Goudie, 2009; Karanasiou *et al.*, 2012; Rezazadeh *et al.*, 2013; Almasi *et al.*, 2014; Goudie, 2014; Diaz *et al.*, 2017; Middleton, 2017). The dominant sources of SDS are originated in the Northern Hemisphere forming the so called "Afro-Asian belt", which includes the west coast of Africa, Middle East, Iran, Afghanistan, Pakistan, Mongolia, and China (Middleton 1986a, b; Herman *et al.*, 1997; Torres *et al.*, 1998; Prospero *et al.*, 2002; Furman *et al.*, 2003; Léon and Legrand, 2003; Goudie, 2009).

Recently, Gherboudj *et al.* (2017) characterized the spatiotemporal variability of the Middle East and North African Dust Emission Potential (MENA-DEP) according to three scales: low dust emission areas, moderate dust emission areas, and high dust emission areas. As such, the high and moderate dust emission areas in north Africa were: Chad, Niger, Mauritania, Occidental Sahara, west and north Algeria, south Tunisia, north-west and central Libya, central Egypt, Sudan, and African horn. In the Middle East, the high and moderate dust emission areas were Jordan, Syria, east Iraq, and Arabian Peninsula. In addition to these areas, central Iran, west Afghanistan, south-west Pakistan, and west India. In spite of these reviews there is a need of investigating the impact on air quality and health of desert dust in different areas by applying comparable methodologies in order to characterize exposure (Querol *et al.*, 2019).

The dust source areas in the Levant, Arabian Peninsula, and Iran were also identified and investigated in several previous studies (Rezazadeh *et al.*, 2013; Alam *et al.*, 2014; Nabavi *et al.*, 2016; Naimabadi *et al.*, 2016; Khaniabadi *et al.*, 2017; Rashki *et al.*, 2017). Al-Dousary *et al.* (2017) classified SDS episodes in the northeast of the Arabian Peninsula during 2000–2017; they distinguished three major types and twelve subtypes of dust storms trajectories based in the width and the shape of the dust outbreak.

The Eastern Mediterranean region also suffers from SDS episodes, which have been reported more frequently during the past decades (Furman *et al.*, 2003; Keramat *et al.*, 2011; Hussein *et al.*, 2011; Hamidi *et al.*, 2013; Hussein *et al.*, 2014; Kchih *et al.*, 2015; Hussein *et al.*, 2017; Munir *et al.*, 2017; Hussein *et al.*, 2018; Bin Abdulwahed *et al.*, 2019; Amarloei *et al.*, 2019; Saeifar *et al.*, 2019; Fountoukis *et al.*, 2020). The increased frequency of SDS episodes in the Eastern Mediterranean region has been referred to the impact of climate change and its consequences by desertification, deforestation, wetland destruction, increased population growth and anthropogenic emissions, food insecurity, and water shortage (Amiraslani and Dragovich 2011; Rezazadeh *et al.*, 2013; Notaro *et al.*, 2015). Notaro *et al.* (2015) showed that the Eastern Mediterranean region has suffered of warming and a drying episode since the beginning of this century. This led to an increased potential to collapse the Fertile Crescent (namely Iraq and Syria). In the Middle East, and especially in the Arabian Peninsula, a pronounced variability in dust activity was reported with an abrupt regime shift from an inactive dust period (1998–2005) to an active dust period (2007–2013) (Aba *et al.*, 2018), which was linked to climate change and global warming impacts in the 2000s (Notaro *et al.*, 2015; Doronzo *et al.*, 2016, 2018). The increased dust episodes and atmospheric dust concentrations on top of the atmosphere have a significant impact on the albedo and short-wave radiation over the African and Arabian regions leading to higher surface reflection (Satheesh *et al.*, 2006), especially in Palestine (Singer *et al.*, 2003), Iraq (Al-Hemoud *et al.*, 2020), Kuwait (Al-Dousari 2009). This also has a socioeconomic impact on oil sector (Al-Hemoud *et al.*, 2019), photovoltaic energy efficiency (Al-Dousari *et al.*, 2019), and health (Al-Dousari *et al.*, 2018). For example, aerosol dust cause direct and indirect adverse effects for fauna, flora and human health in the regional scale (Abd El-Wahab *et al.*, 2018).

Besides climate change impacts, anthropogenic aerosols have had an increasing trend during the previous decades in the Middle East (Givati and Rosenfeld, 2007). These particles are anticipated to slow down the conversion of cloud drops into raindrops and snowflakes, thus decreasing precipitation from short-lived clouds such as form in moist air that crosses topographic barriers. This in turn, escalated the desertification process in the Middle East causing increased frequency of dust episodes and atmospheric dust particle concentrations.

While aerosol research has been given increased attention in the Eastern Mediterranean, it is still at an early stage in the Middle East (Hamad *et al.*, 2015; Heo *et al.*, 2017; Taheri *et al.*, 2019), especially in Jordan (Hussein *et al.*, 2018). Therefore, the main objective of this study was to investigate the particulate matter (PM_{10} and $PM_{2.5}$) mass concentrations over a long-term period from May 2018 to March 2019 in the urban atmosphere of Amman, Jordan. The methods included aerosols sampling using high-volume samplers and gravimetric analysis combined with air mass back trajectories to identify the source origin of SDS episodes.

METHODS

Measurement Location

The long-term aerosol measurement campaign was performed during May 2018–March 2019 on the roof top (about 20 m above the ground) of the Department of Physics at the campus of the University of Jordan [32.0129N, 35.8738E]. The campus is situated at an urban background location in the northern part of Amman, which is the capital city of Jordan. The surrounding area of the campus is a mixture of residential area and road network with one of the main roads (Queen Rania street) passing parallel to the west side of the campus (Fig. S1). The downtown was about 10 km south of the campus area.

High-volume Sampling

Two high-volume samplers (model CAV-A/mb, MCV, S.A., Spain) were used; one for PM_{10} and another one for $PM_{2.5}$. The high-volume samplers were operated at 30 $m^3 h^{-1}$ and record the overall mean temperature and pressure during the sampling session. The cascade heads (model PM1025-CAV, MCV, S.A.) were used for sampling particles with aerodynamic diameter lower than 10 µm (PM_{10}) and lower than 2.5 µm ($PM_{2.5}$) respectively. These sampling heads can accommodate a 15-centimetre diameter round filters, which were quartz filters (Pallflex, PALLXQ250ETDS0150, TISSUQUARTZ 2500 QAT-UP).

Each sampling session (including PM_{10} and $PM_{2.5}$) lasted for 24-hours every 6 days. In total, 51 PM_{10} samples and 48 $PM_{2.5}$ samples were collected. Blank sampling was performed several times during the campaign by following the same procedure as for the active sampling except that the high-volume sampler was turned off (i.e., zero flow rate). The blank samples were necessary for the accuracy check of the sampling procedure and analysis (Querol *et al.*, 2004).

Gravimetric Analysis

The gravimetric analysis was according to the European directive EN1234-1 (20°C and 50% HR) at the Institute of Environmental Assessment and Water Research (IDAEA-CSIC, Barcelona, Spain). The gravimetric analysis included pre-sampling and post-sampling weighing of each filter (including blanks). The pre-weighing and post-weighing were done with the same procedure: conditioning temperature 20°C and relative humidity 50%. The conditioning time was 2 days. Each sample was weighed twice (24 hours interval in between) and the average value was recorded. The weighing was made by using a microbalance (Mettler-Toledo, model: XP105 with electrostatic charge detection, Switzerland).

The 24-hour average particulate matter concentration (PM_x [µg m^{-3}]) was calculated

$$PM_x = \frac{m_{psot} - m_{pre}}{Q \times \Delta t} \quad (1)$$

where m_{post} and m_{post} [µg] are the post sampling and the pre-sampling weight of the filter, Q [30 m^3 h^{-1}] is the sampling flow rate, and Δt [24 hours] is the sampling time interval.

Meteorological Conditions

The weather conditions were monitored on-site with a weather station (WH-1080, Clas Ohlson: Art. no. 36-3242), which was set to record the reading with 5-minute interval. The weather data included: ambient temperature, pressure, relative humidity, wind speed and direction, and precipitation.

Back Trajectories

Air mass back trajectories were calculated by using the Hybrid Single Particle Lagrangian Integrated Trajectory (HYSPLIT) model (Draxler and Hess, 1997; Draxler *et al.*, 2012; Stein *et al.*, 2015), which provides detailed information about the origin and path of air masses that arrived at the measurement site. Four-days back trajectories were calculated for each hour at arrival heights 100, 500, and 1500 meters above ground level.

Back trajectories crossing maps were generated in terms of the frequency of air mass crossing over each grid cell of the domain. Here the domain was taken to cover the west-south Asia, North Africa, and Europe (i.e., longitude –20°–60° and latitude 15°–55°). The crossing map resolution was set to 0.5° for the 4-day back trajectories calculated for each hour.

RESULTS AND DISCUSSION

Meteorological Conditions

The hourly, daily, and monthly means of the meteorological conditions (ambient temperature (T), relative humidity (RH), absolute pressure (P), wind speed (WS), and hourly precipitation) are presented in Fig. 1. The monthly mean, standard deviation, minimum, and maximum values are listed in Table S2.

The ambient temperature (T) showed a clear seasonal variation with high values during the summer (June–August) and low values during the winter (December–February). During the summer, the monthly mean T was around 24°C and during the winter it was around 9°C (Fig. 1(a)). During May 2018–March 2019, the daily mean T was in the range 3–30°C (overall mean 17 ± 7°C).

The seasonal variation of the relative humidity (RH, Fig. 1(b)) and the absolute pressure (P, Fig. 1(c)) was opposite to that of T. For example, the monthly RH was about 55% and 82% during the summer and the winter; respectively. As for P, it was about 896 hPa and 901 hPa during the summer and the winter; respectively. During May 2018–March 2019, the daily mean RH was in the range 20–100% (overall mean 68 ± 21%) and the daily mean P was in the range 890–908 hPa (overall mean 899 ± 4 hPa).

The wind speed (WS) showed a different monthly variation than T, RH, and P. The monthly mean wind speed was minimum during the autumn (September–November) and maximum during the summer (Fig. 1(d)). The maximum monthly WS value was about 2.1 m s^{-1} (August) and the minimum was about 0.8 m s^{-1} (November). During May 2018–March 2019, the maximum daily mean WS was about 3.6 m s^{-1} (March 1, 2019).

The rain season started in October 2018 with a small amount (cumulative ~13 mm) (Fig. 1(e)). During December 2018, the cumulative precipitation was about 180 mm. During January–February 2019, the cumulative precipitation was about 120 mm. By the end of the measurement campaign (i.e., March 2019), the cumulative precipitation was about 470 mm.

Back Trajectories

The 4-day back trajectories crossing maps are presented in Fig. S2 (Supplementary Material) for arrival heights 100 m and 1500 m. The spatial extent of the trajectories crossing for 1500 m arrival height was broader than that for 100 m arrival height. For back trajectories arrived at 1500 m height, they covered the whole Mediterranean Sea Basin and included north Africa, Red Sea, north and middle region of the Arabia Peninsula, the Levant with an extension to the Caspian Sea, and Europe. As for arrival height at 100 m, the back trajectories covered the middle and eastern parts of the Mediterranean Sea, northeast Africa, north Red Sea, north Arabian Peninsula, the Levant, and southeast Europe. Furthermore, trajectories arrived at 100 m showed a predominant crossing path over the eastern part of the Mediterranean Sea.

Particulate Matter (PM) Concentrations

Throughout the measurement period (Fig. 2 and Table S3), the PM_{10} daily concentration varied between 20

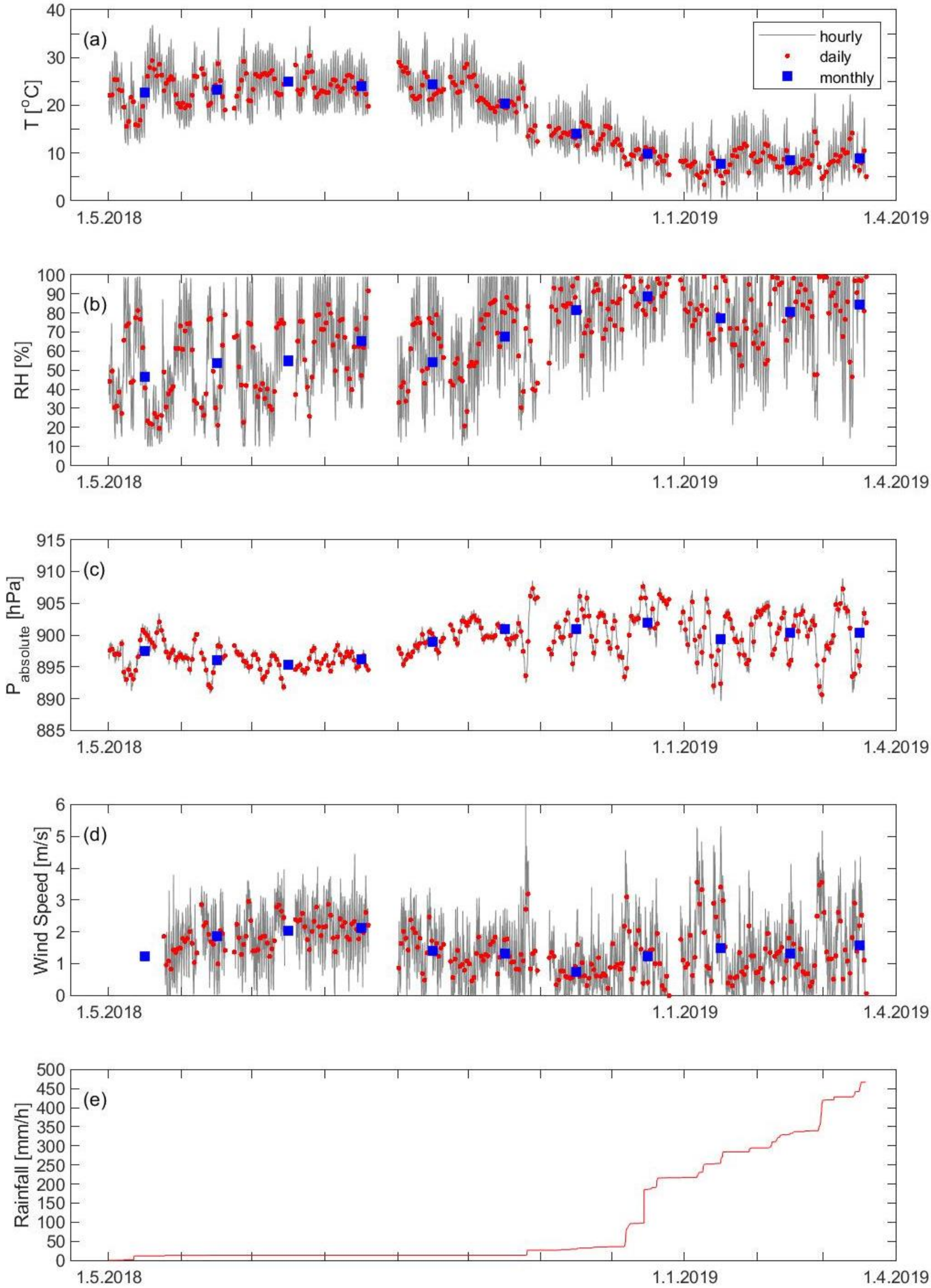

Fig. 1. Time series of weather conditions during May 1, 2018–March 19, 2019 presented as hourly, daily, and monthly means for (a) ambient temperature, (b) relative humidity, (c) absolute pressure, and (d) wind speed. (e) The rainfall was presented as hourly cumulative precipitation.

and 190 µg m^{-3} with an overall average 64 ± 39 µg m^{-3}. The $PM_{2.5}$ daily concentration varied between 15 and 190 µg m^{-3} with an overall average 47 ± 32 µg m^{-3} (i.e., annual). The ratio $PM_{2.5}/PM_{10}$ was more than 0.4 and the overall mean was 0.8 ± 0.2; i.e., about 80% of the PM_{10} was within the fine fraction (Fig. 2 and Table S3).

Surprisingly, the PM concentrations did not show a clear seasonal variation. This is contrary to previous observation reported via on-line continuous long-term measurement of the particle number size distribution, which showed a clear seasonal variation for the coarse mode particle number concentration with higher concentrations during the winter than summer and showed specific peaks in spring and autumn (Hussein *et al.*, 2018, 2019). A reason for not observing this seasonal variation in this study can be due to the sampling protocol conducted here; collecting a sample every 6 days. Therefore, it is recommended to perform the sampling every other day if not possible on daily basis; i.e., higher time resolution of the sampling sessions is recommended.

According to the Jordanian standards (JS-1140/2006) for ambient air quality, the annual mean the PM_{10} and $PM_{2.5}$ must not exceed 70 µg m^{-3} and 15 µg m^{-3}; respectively. This means that the observed PM_{10} annual mean value is below its annual limit value but the $PM_{2.5}$ annual mean three times higher than its limit value. As for the 24 h mean limit value, PM_{10} and $PM_{2.5}$ must not exceed 120 µg m^{-3} and 65 µg m^{-3}; respectively. According to this, the exceedance of PM_{10} was 6 times and that of $PM_{2.5}$ was 7 times. As will be shown in the next section, these exceedances were during the reported SDS episodes. Compared to the World Health Organization (WHO) air quality guidelines for PM_{10} (annual and 24h must not exceed 20 µg m^{-3} and 50 µg m^{-3}; respectively) and $PM_{2.5}$ (annual and 24h must not exceed 10 µg m^{-3} and 25 µg m^{-3}; respectively), the observed annual concentrations here are exceeded both annual guidelines. According to the 24 h WHO guidelines, only 6 days did not exceed the $PM_{2.5}$ limit value and 25 days did not exceed the PM_{10} limit value.

The WHO (2018) released an update for the global ambient air quality database that reported the annual mean PM_{10} and $PM_{2.5}$ concentrations during 2008–2016. Recalling the data for three Jordanian cities (Al-Zarqa', Amman, and Irbid) in 2017, the annual mean PM_{10} was 82, 68, and 53 µg m^{-3}; respectively. This is consistent with our observation here with an annual mean PM_{10} ~64 µg m^{-3}. The world overall annual mean PM_{10} was ~72 µg m^{-3} during 2008–2016, which is slightly higher than what was observed during our measurement campaign.

In general, the annual mean PM_{10} concentrations in Jordan were higher than what was reported by the WHO (2018) in urban, suburban, and residential sites in countries around the Mediterranean Sea in 2016. For example, the annual mean PM_{10} for Turkish cities (80 sites) was 52 ± 18 µg m^{-3} (range 17–91 µg m^{-3}), Italian cities (231 sites) was about 25 ± 6 µg m^{-3} (range 10–43 µg m^{-3}), Greek cities (12 sites) was 52 ± 18 µg m^{-3} (range 21–43 µg m^{-3}), Cypriot cities (4 sites) was 37 ± 6 µg m^{-3} (range 29–41 µg m^{-3}), and two Maltese cities 38 ± 8 µg m^{-3} (range 32–43 µg m^{-3}).
Compared to other cities in the Middle East as reported by the WHO (2018), the annual mean PM_{10} concentrations in Jordan were lower than what was observed in Kuwait (130 ± 35 µg m^{-3}; 9 sites), Palestine and Israel (90 µg m^{-3}), Egypt (249–284 µg m^{-3}; two sites), and the United Arab of Emirates (122–153 µg m^{-3}; three sites).

Sand and Dust Storm (SDS) Episodes

As indicated in Fig. 2, SDS episodes were considered when PM_{10} > 70 µg m^{-3}. This arbitrary threshold was selected based on the distribution of daily PM_{10} concentrations, which showed two distinct groups of samples below and above this threshold (Fig. S3 in Supporting Material). In practice, this threshold is slightly higher than the annual PM_{10} mean value and it separates two groups of the PM_{10} concentrations distributions. Based on this threshold, 14 days were identified and listed in Table 1. According to the air mass back trajectories analysis, the atmospheric SDS was transported from three main source regions: (1) long-range transport from north Africa (Sahara), (2) medium range transport from the Arabian Peninsula, and (3) short-range transported from the Levant. Sometimes, the transport was a combination of two or three regions. Accordingly, type identification was suggested: S-type originated from Sahara region, SL-type originated from Sahara region and the Levant region (i.e., SDS combined from these two regions), and SLA-type originated from all three regions. The SLA was the most common SDS type because the back trajectories originated from north Africa crosses or circulates over the northern part of the Arabian Peninsula and the Levant region.

During the measurement period, a single S-type SDS episode (on July 25, 2018; PM_{10} ~121 µg m^{-3} and $PM_{2.5}$ ~109 µg m^{-3}) was identified, which was solely originated from the Sahara region (Fig. 3). Interestingly, during this episode the back trajectories arrived at 1500 m (Fig. 3(c)) were originated and crossed over North Africa but those arrived at 100 m and 500 m (Figs. 3(a)–3(b)) were from the Mediterranean Sea.

Two SL-type SDS episodes were identified (Table 1) when the air masses originated from the Sahara region and circulated over the Levant region (Fig. 4). During these episodes, the back trajectories arrived at 100 m and 500 m originated from the Mediterranean Sea and circulated over the western parts of Syria, but the trajectories arrived at 1500 m circulated originated from the Sahara region and circulated over Syria, Iraq, and Jordan (i.e., Levant). During the first SL-type episode (May 26, 2018) the PM_{10} concentration was about 108 µg m^{-3} and during the second one (June 7, 2018) it was about 127 µg m^{-3}. The average for SL-type episodes was 117 µg m^{-3} and 112 µg m^{-3} for PM_{10} and $PM_{2.5}$, respectively, with a $PM_{2.5}/PM_{10}$ ratio of 0.95. The fine size distribution measured during the S and SL types, can be due to size segregation during transport with preferential deposition of coarser particles.

During the autumn, winter, and spring, more intense SDS episodes were observed and they spanned over long time periods (Table 1). These episodes SLA-type SDS (Fig. 5). The back trajectories analysis at all arrival heights confirmed the origin of these SDS to be from the three regions dust sources: Sahara, Arabian Peninsula, and Levant. During these SLA-type episodes, the PM_{10} concentration was in the range 88–188 µg m^{-3}. An intensive SLA-type episode was observed during several weeks in October, 2018 (Fig. 2). During this episode, the PM_{10} concentrations were higher than 100 µg m^{-3} and also recorded the highest concentration (as high as 188 µg m^{-3}). The average for SLA-type episodes was 122 µg m^{-3} and 77 µg m^{-3} for PM_{10} and $PM_{2.5}$, respectively, with a $PM_{2.5}/PM_{10}$ ratio of 0.63. The coarser size distribution of PM during the SLA types compared with the S and SL

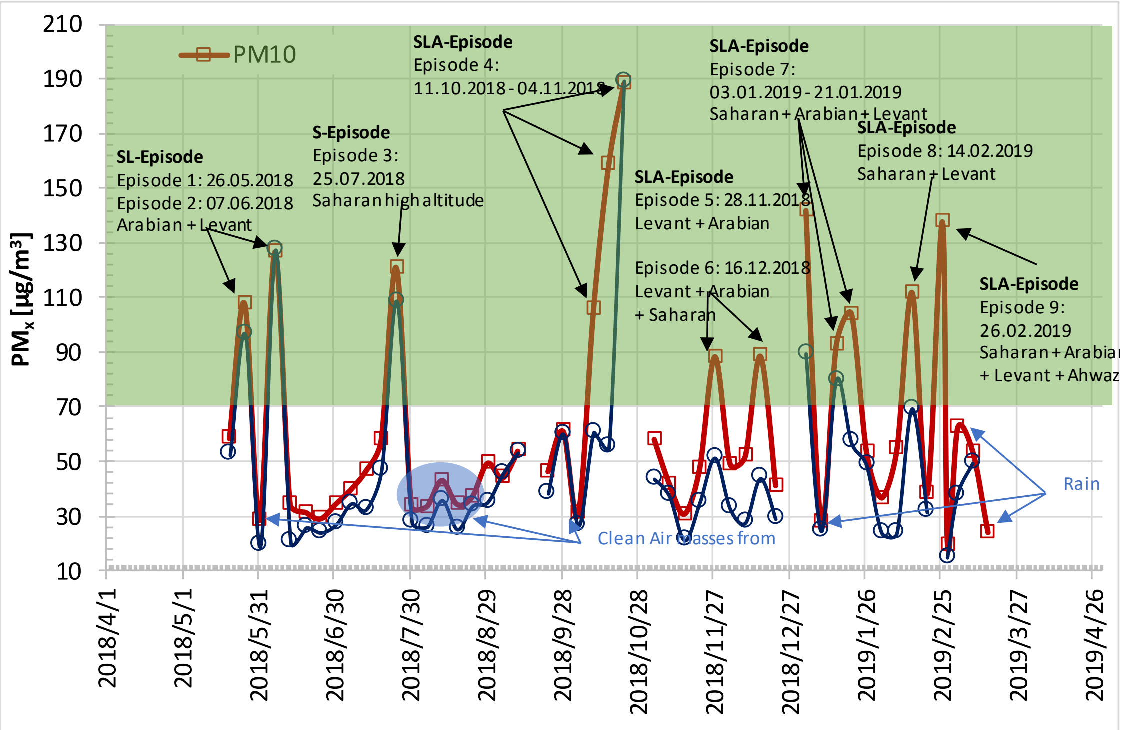

Fig. 2. Time series of PM_{10} and $PM_{2.5}$ concentrations with markups for sand and dust episodes (SDS) and clean air periods (i.e., PM_{10} concentrations < 70 µg m^{-3}).

Table 1. Sand and Dust Storm (SDS) episodes according to type and observation during the sampling period. The type of SDS is denoted as: Saharan (S); Saharan and Levant (SL); Saharan, Arabian, and Levant (SAL); Saharan, Arabian, Levant, and Ahvaz (SALA). The source region was verified according to the back trajectories analysis for crossing maps on the sampling day (+ following day). The date here indicates the start of the sampling day.

SDS Type	Source Region	Dates	PM_{10} (µg m^{-3})
S	Saharan	25-07-2018	120.9
SL	Saharan and Levant	26-05-2018	107.8
		07-06-2018	126.7
SLA	Saharan, Levant, and Arabian	11-10-2018	105.7
		17-10-2018	158.6
		23-10-2018	188.3
		28-11-2018	88.3
		16-12-2018	88.5
		03-01-2019	141.9
		15-01-2019	92.6
		21-01-2019	104.0
		14-02-2019	111.8
		26-02-2019	137.7
CLEAN	Eastern Mediterranean Sea	01-06-2018	28.4
		31-07-2018	33.4
		06-08-2018	33.3
		12-08-2018	43.0
		18-08-2018	34.2
		24-08-2018	36.9
		28-02-2019	19.3

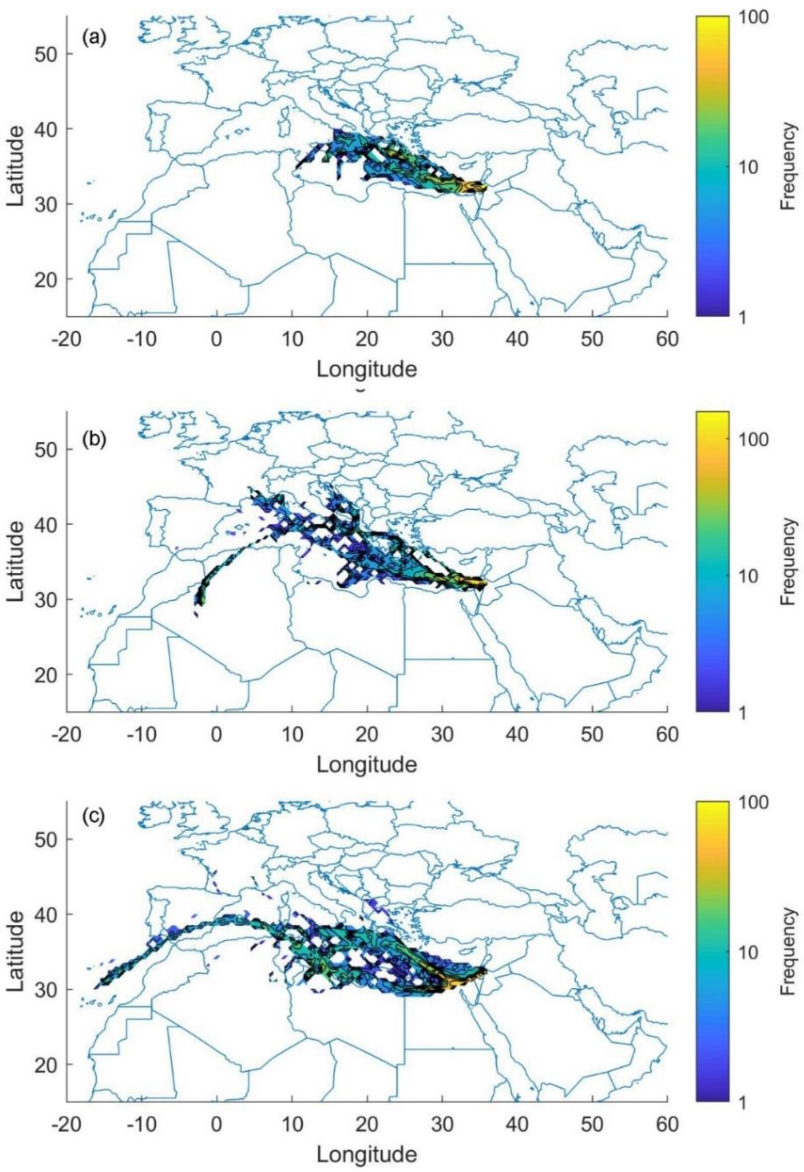

Fig. 3. Back trajectories (96 hours) crossing maps during S-type SDS-episodes (indicated on Fig. 2) at arrival heights (a) 100 meters, (b) 500 meters, and (c) 1500 meters. The arrival location was the campus of the University of Jordan, Amman, Jordan. These maps were generated from the hourly back trajectories during the sampling dates (+ following day).

types, is probably due the proximity of the source area.

Notice that S-type and SL-type episodes occurred during the summer. They indicate that some SDS episodes can be lifted up to the upper atmosphere while being transported from their source region to the receptor region, where they settle down. The SLA-type episodes occurred during the Autumn, winter, and spring and they recorded higher PM_{10} concentrations than the S-type and SL-type episodes, which occurred in the summer. Furthermore, SLA-type episodes transported dust at any arrival height and the back trajectories crossed over a larger spatial extent than that for the S-type and SL-type episodes.

As a comparison to the SDS days, the PM_{10} concentrations less than 50 µg m^{-3} occurred during rainy days or accompanied with air masses originating and crossing over the Mediterranean Sea and the eastern part of Europe (Table 1, Fig. 2, Fig. 6).

Sahara SDS crossing over the Mediterranean Sea was reported in the literature (Gkikas *et al.*, 2018; Solomos *et al.*, 2018). Solomos *et al.* (2018) analyzed a record-breaking dust episode observed on Crete on March 22, 2018 that recorded 24h mean PM_{10} concentration as 206, 850, and 1125 µg m^{-3} in Chania, Finokalia, and Heraklion; respectively.

Gkikas *et al.* (2018) focused on the direct radiative effects of 20 intense and widespread dust outbreaks originated in North Africa and affected the Mediterranean basin during March 2000–February 2013. Similarly, Alam *et al.* (2014) and Nabavi *et al.* (2016) focused on the aerosol optical depth and climatology of some dust outbreaks originated in the Middle East and the Arabian Peninsula that affected west-south Asia. According to these studies, the dust transport in the Middle East and North Africa (MENA) region is transported

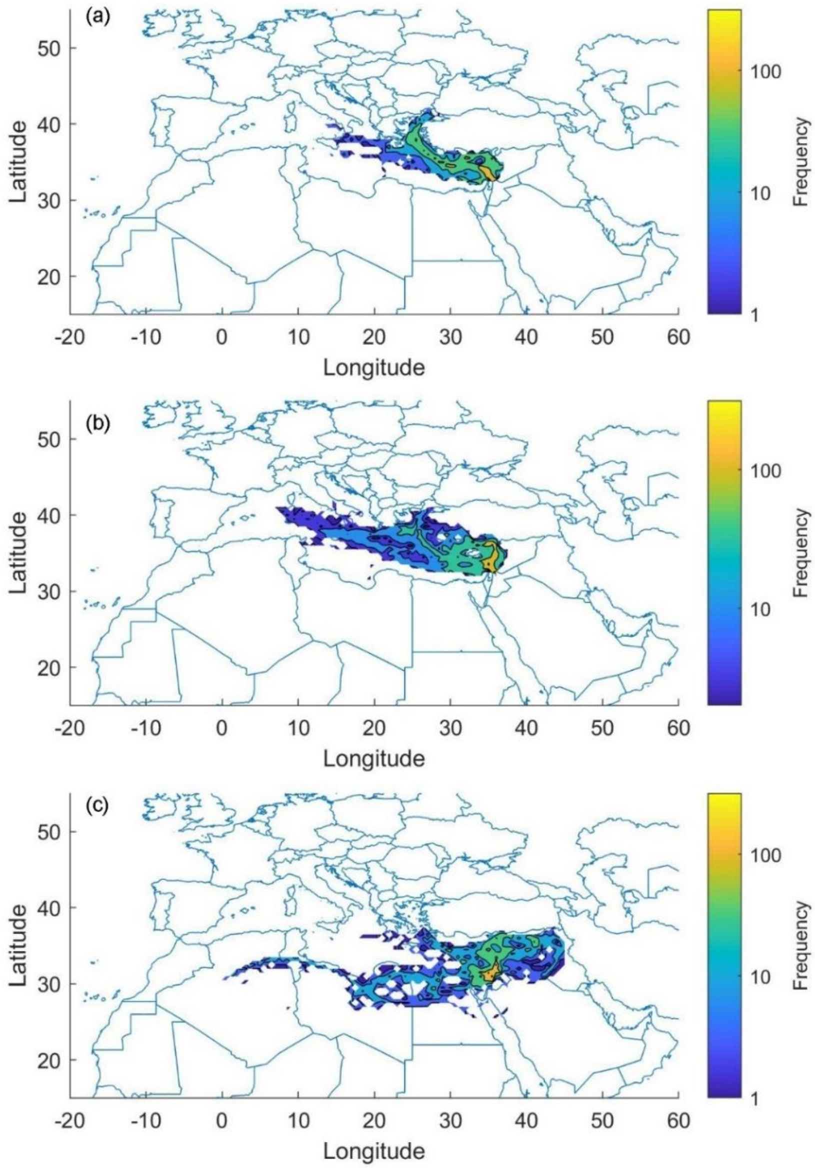

Fig. 4. Back trajectories (96 hours) crossing maps during SL-type SDS-episodes (indicated on Fig. 2) at arrival heights (a) 100 meters, (b) 500 meters, and (c) 1500 meters. The arrival location was the campus of the University of Jordan, Amman, Jordan. These maps were generated from the hourly back trajectories during the sampling dates (+ following day).

from west to east (Alam *et al.*, 2014; Nabavi *et al.*, 2016; Naimabadi *et al.*, 2016; Khaniabadi *et al.*, 2017; Rashki *et al.*, 2017; Gkikas *et al.*, 2018). This consistent with previous observation in Jordan that most of the SDS was mainly started from North Africa and transported to the Middle East after crossing/circulating over the Arabian Peninsula and the Levant. Nevertheless, some episodes started within the Levant and the southern region of the Arabian Peninsula.

CONCLUSIONS

Air quality issues related to sand and dust storms (SDS) in the Middle East are one of the critical issues that require more attention because the frequency and the intensity of SDS episodes have increased recently due to escalating climate change impacts and increased anthropogenic emissions in the region. Here, particulate matter (PM_{10} and $PM_{2.5}$) concentrations were measured and investigated during May 2018–March 2019 in the urban atmosphere of Amman, Jordan. The methods included aerosols sampling using high-volume samplers and gravimetric analysis combined with air mass back trajectories.

The annual mean PM_{10} concentration was 64 ± 39 µg m^{-3} (20–190 µg m^{-3}). The $PM_{2.5}/PM_{10}$ ratio was 0.8 ± 0.2, which means that about 80% of the PM_{10} was within the fine fraction. According to the Jordanian Air Quality standards (JS-1140/2006), the observed PM_{10} annual mean value was below its limit value but that of the $PM_{2.5}$ was three times higher than its limit value. However, both exceeded the World Health Organization (WHO) air quality guideline. According to the WHO global ambient air quality database during 2008–2016, the annual mean PM_{10} concentrations in

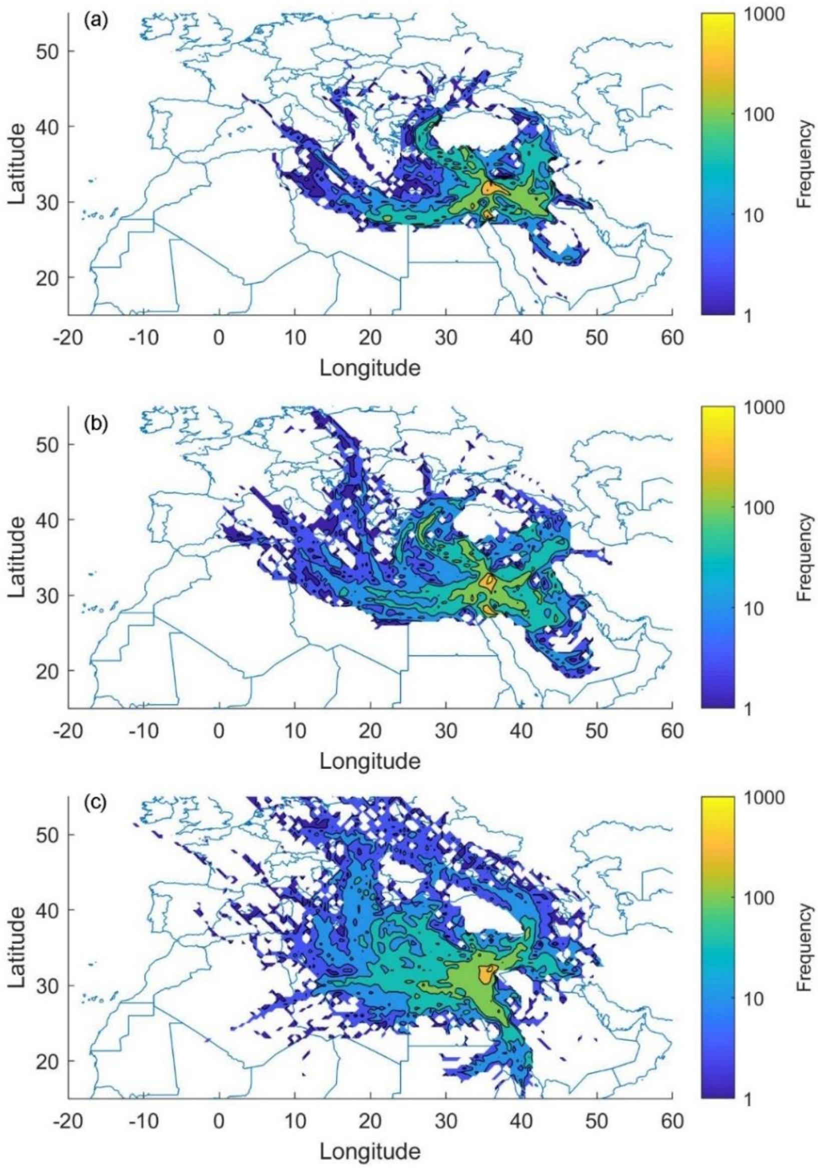

Fig. 5. Back trajectories (96 hours) crossing maps during SLA-type SDS-episodes (indicated on Fig. 2) at arrival heights (a) 100 meters, (b) 500 meters, and (c) 1500 meters. The arrival location was the campus of the University of Jordan, Amman, Jordan. These maps were generated from the hourly back trajectories during the sampling dates (+ following day).

Jordan were lower than what was reported for other cities in the Middle East but were higher when compared to other Mediterranean cities.

During the measurement period extending over 11 months, Jordan was affected by SDS episodes on 14 days. The source origins of these dust outbreaks were traced back to North Africa, the Arabian Peninsula, and the Levant. The 24-hour PM_{10} concentrations during these SDS episodes ranged between 108 µg m^{-3} and 188 µg m^{-3}, which is about 3–6 times higher than the mean values during clean conditions (~33 µg m^{-3}).

The limitation of this study is the sampling protocol as collecting a 24-hour sample every 6 days. It is recommended to perform the sampling with higher time resolution. In the future, we continue monitoring with this method and also include on/line sampling with an optical particle sizer. Combining ground-based monitoring with satellite observation would provide an insight into the SDS episodes characteristics and calibration of the satellite observations.

ACKNOWLEDGMENTS

This research was part of a close collaboration between the University of Jordan, Institute of Environmental Assessment and Water Research (IDAEA-CSIC), and the Institute for Atmospheric and Earth System Research (INAR / Physics, University of Helsinki). We acknowledge financial support provided by the Deanship of Academic Research (DAR, project No. 2015) at the University of Jordan, the Spanish Ministry of Science and Innovation (Project CEX2018-000794-S) and by AGAUR (project 2017 SGR41), and Academy of Finland Center of Excellence (project.

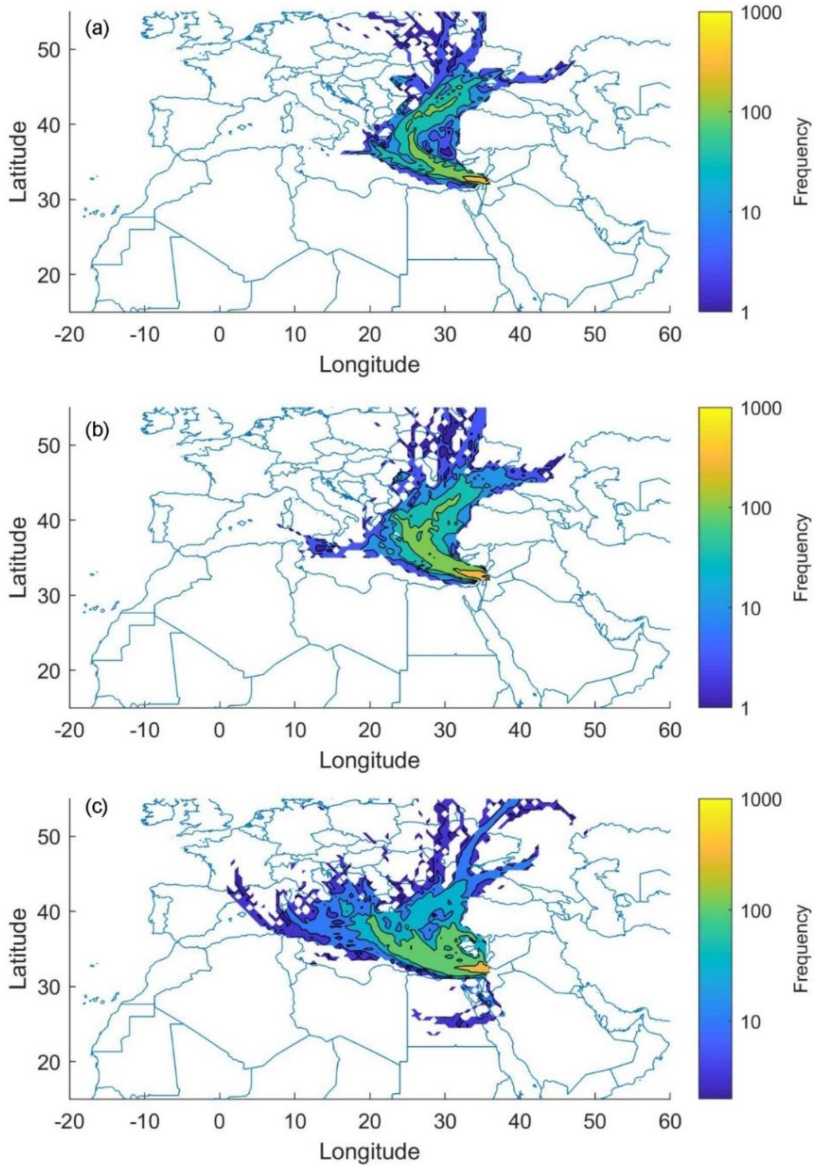

Fig. 6. Back trajectories (96 hours) crossing maps during low PM_{10} concentrations (indicated on Fig. 2) at arrival heights (a) 100 meters, (b) 500 meters, and (c) 1500 meters. The arrival location was the campus of the University of Jordan, Amman, Jordan. These maps were generated from the hourly back trajectories during the sampling dates (+ following day).

No 272041), ERA-PLANET (www.era-planet.eu), trans-national project SMURBS (grant n. 689443 EU Horizon 2020 Framework Programme and Academy of Finland via the Center of Excellence in Atmospheric sciences and NanoBioMass (project number 1307537). The eCOST action (inDUST, project number CA16202) is acknowledged for supporting this research via the Short Term Scientific Mission (STSM) mobility grant. This manuscript was written and completed during the sabbatical leave of the first author (Tareq Hussein) that was spent at the University of Helsinki and supported by the University of Jordan during 2019.

DISCLAIMER

The authors declare no conflict of interest.
Data will be available upon request.

SUPPLEMENTARY MATERIAL

Supplementary data associated with this article can be found in the online version at https://doi.org/10.4209/aaqr.2020.05.0195

REFERENCES

Aba, A., Al-Dousari, A.M. and Ismaeel, A. (2018). Atmospheric deposition fluxes of ^{137}Cs associated with dust fallout in the northeastern Arabian Gulf. *J. Environ. Radioact.* 192: 565–572. https://doi.org/10.1016/j.jenvrad.2018.05.010

Abd El-Wahab, R.H., Al-Rashed, A.R. and Al-Dousari, A. (2018). Influences of physiographic factors, vegetation patterns and human impacts on aeolian landforms in arid environment. *Arid Ecosyst.* 8: 97–110. https://doi.org/10.1134/S2079096118020026

Alam, K., Trautmann, T., Blaschke, T. and Subhan, F. (2014). Changes in aerosol optical properties due to dust storms in the Middle East and Southwest Asia. *Remote Sens. Environ.* 143: 216–227. https://doi.org/10.1016/j.rse.2013.12.021

Al-Dousari, A.M. (2009). Section III: Recent studies on dust fallout within preserved and open areas in Kuwait. Desertification in arid lands: Causes, consequences and mitigation. KUWAIT. J. SCI. pp. 137–148.

Al-Dousari, A., Doronzo, D. and Ahmed, M. (2017). Types, indications and impact evaluation of sand and dust storms trajectories in the Arabian Gulf. *Sustainability* 9: 1526. https://doi.org/10.3390/su9091526

Al-Dousari, A.M., Ibrahim, M. I., Al-Dousari, N., Ahmed, M. and Al-Awadhi, S. (2018). Pollen in aeolian dust with relation to allergy and asthma in Kuwait. *Aerobiologia* 34: 325–336. https://doi.org/10.1007/s10453-018-9516-8

Al-Dousari, A., Al-Nassar, W., Al-Hemoud, A., Alsaleh, A., Ramadan, A., Al-Dousari, N. and Ahmed, M. (2019). Solar and wind energy: Challenges and solutions in desert regions. *Energy* 176: 184–194. https://doi.org/10.1016/j.energy.2019.03.180

Al-Hemoud, A., Al-Dousari, A., Misak, R., Al-Sudairawi, M., Naseeb, A., Al-Dashti, H. and Al-Dousari, N. (2019). Economic impact and risk assessment of sand and dust storms (SDS) on the oil and gas industry in Kuwait. *Sustainability* 11: 200. https://doi.org/10.3390/su11010200

Al-Hemoud, A., Al-Dousari, A., Al-Dashti, H., Petrov, P., Alsaleh, A., Al-Khafaji, S., Behbehani, W., Li, J. and Koutrakis, P. (2020). Sand and dust storm trajectories from Iraq Mesopotamian flood plain to Kuwait. *Sci. Total Environ.* 710: 136291. https://doi.org/10.1016/j.scitotenv.2019.136291

Almasi, A., Mousavi, A. R., Bakhshi, S. and Namdari, F. (2014). Dust storms and environmental health impacts. *J. Middle East Appl. Sci. Technol.* 8: 353–356. https://jmeast.webs.com/JMEAST-%20P001,%20Sup-issue%208,%202014.pdf

Amarloei, A., Fazlzadeh, M., Jafari, A. J., Zarei, A. and Mazloomi, S. (2020). Particulate matters and bioaerosols during Middle East dust storms events in Ilam, Iran. *Microchem. J.* 152: 104280. https://doi.org/10.1016/j.microc.2019.104280

Amiraslani, F. and Dragovich, D. (2011). Combating desertification in Iran over the last 50 years: An overview of changing approaches. *J. Environ. Manage.* 92: 1–13. https://doi.org/10.1016/j.jenvman.2010.08.012

Bin Abdulwahed, A., Dash, J. and Roberts, G. (2019). An evaluation of satellite dust-detection algorithms in the Middle East region. *Int. J. Remote Sens.* 40: 1331–1356. https://doi.org/10.1080/01431161.2018.1524589

Díaz, J., Linares, C., Carmona, R., Russo, A., Ortiz, C., Salvador, P. and Trigo, R.M. (2017). Saharan dust intrusions in Spain: Health impacts and associated synoptic conditions. *Environ. Res.* 156: 455–467. https://doi.org/10.1016/j.envres.2017.03.047

Doronzo, D.M., Khalaf, E. A., Dellino, P., de Tullio, M. D., Dioguardi, F., Gurioli, L., Mele, D., Pascazio, G. and Sulpizio, R. (2015). Local impact of dust storms around a suburban building in arid and semi-arid regions: Numerical simulation examples from Dubai and Riyadh, Arabian Peninsula. *Arab. J. Geosci.* 8: 7359–7369. https://doi.org/10.1007/s12517-014-1730-2

Doronzo, D.M., Al-Dousari, A., Folch, A. and Dagsson-Waldhauserova, P. (2016). Preface to the dust topical collection. *Arab. J. Geosci.* 9: 468. https://doi.org/10.1007/s12517-016-2504-9

Doronzo, D.M. and Al-Dousari, A. (2019). Preface to dust events in the environment. *Sustainability* 11: 628. https://doi.org/10.3390/su11030628

Draxler, R. and Hess, G.D. (1997). Description of the HYSPLIT_4 modeling system, NOAA Tech. Memo. ERL ARL-224: Maryland, MD, USA. https://www.arl.noaa.gov/wp_arl/wp-content/uploads/documents/reports/arl-224.pdf (accessed December 1, 2020).

Draxler, R., Stunder, B., Rolph, G., Stein, A. and Taylor, A. (2020). HYSPLIT4 User's Guide. http://www.arl.noaa.gov/documents/reports/hysplit_user_guide.pdf (accessed on 08.01.2020).

Evan, A.T., Foltz, G.R., Zhang, D. and Vimont, D.J. (2011). Influence of African dust on ocean–atmosphere variability in the tropical Atlantic. *Nat. Geosci.* 4: 762–765. https://doi.org/10.1038/ngeo1276

Fountoukis, C., Harshvardhan, H., Gladich, I., Ackermann, L. and Ayoub, M.A. (2020). Anatomy of a severe dust storm in the Middle East: Impacts on aerosol optical properties and radiation budget. *Aerosol Air Qual. Res.* 20: 155–165. https://doi.org/10.4209/aaqr.2019.04.0165

Furman, H.K.H. (2003). Dust storms in the Middle East: Sources of origin and their temporal characteristics. *Indoor Built Environ.* 12: 419–426. https://doi.org/10.1177/1420326X03037110

Gherboudj, I., Beegum, S.N. and Ghedira, H. (2017). Identifying natural dust source regions over the Middle-East and North-Africa: Estimation of dust emission potential. *Earth Sci Rev.* 165: 342–355. https://doi.org/10.1016/j.earscirev.2016.12.010

Gillette, D.A., Blifford Jr, I.H. and Fryrear, D.W. (1974). The influence of wind velocity on the size distributions of aerosols generated by the wind erosion of soils. *J. Geophys. Res.* 79: 4068–4075. https://doi.org/10.1029/JC079i027p04068

Gillette, D.A. and Walker, T.R. (1977). Characteristics of airborne particles produced by wind erosion of sandy soil, high plains of west Texas. *Soil Sci.* 123: 97–110.

Givati, A. and Rosenfeld, D. (2007). Possible impacts of anthropogenic aerosols on water resources of the Jordan River and the Sea of Galilee. *Water Resour. Res.* 43: W10419. https://doi.org/10.1029/2006WR005771

Gkikas, A., Obiso, V., Perez Garcia-Pando, C., Jorba, O., Hatzianastassiou, N., Vendrell, L., Basart, S., Solomos, S., Gassó, S. and Baldasano Recio, J.M. (2018). Direct radiative effects during intense Mediterranean desert dust outbreaks. *Atmos. Chem. Phys.* 18: 8757–8787. https://doi.org/10.5194/acp-18-8757-2018

Goudie, A.S. (2009). Dust storms: Recent developments. *J.*

Environ. Manage. 90: 89–94. https://doi.org/10.1016/j.jenvman.2008.07.007

Goudie, A.S. (2014). Desert dust and human health disorders. *Environ. Int.* 63: 101–113. https://doi.org/10.1016/j.envint.2013.10.011

Hamad, S.H., Schauer, J.J., Heo, J. and Kadhim, A.K. (2015). Source apportionment of $PM_{2.5}$ carbonaceous aerosol in Baghdad, Iraq. *Atmos. Res.* 156: 80–90. https://doi.org/10.1016/j.atmosres.2014.12.017

Hamidi, M., Kavianpour, M.R. and Shao, Y. (2013). Synoptic analysis of dust storms in the Middle East. *Asia Pac. J. Atmos. Sci.* 49: 279–286. https://doi.org/10.1007/s13143-013-0027-9

Heo, J., Wu, B., Abdeen, Z., Qasrawi, R., Sarnat, J.A., Sharf, G., Shpund, K. and Schauer, J.J. (2017). Source apportionments of ambient fine particulate matter in Israeli, Jordanian, and Palestinian cities. *Environ. Pollut.* 225: 1–11. https://doi.org/10.1016/j.envpol.2017.01.081

Herman, J.R., Bhartia, P.K., Torres, O., Hsu, C., Seftor, C. and Celarier, E. (1997). Global distribution of UV-absorbing aerosols from Nimbus 7/TOMS data. *J. Geophys. Res.* 102: 16911–16922. https://doi.org/10.1029/96JD03680

Hoek, G., Krishnan, R.M., Beelen, R., Peters, A., Ostro, B., Brunekreef, B. and Kaufman, J.D. (2013). Long-term air pollution exposure and cardio-respiratory mortality: A review. *J. Environ. Health* 12: 43. https://doi.org/10.1186/1476-069X-12-43

Hussein, T., Al-Ruz, R. A., Petäjä, T., Junninen, H., Arafah, D. E., Hämeri, K. and Kulmala, M. (2011). Local air pollution versus short-range transported dust episodes: A comparative study for submicron particle number concentration. *Aerosol Air Qual. Res.* 11: 109–119. https://doi.org/10.4209/aaqr.2010.08.0066

Hussein, T., Alghamdi, M.A., Khoder, M., AbdelMaksoud, A.S., Al-Jeelani, H., Goknil, M.K., Shabbaj, I.I., Almehmadi, F.M., Hyvarinen, A., Lihavainen, H. and Hämeri, K. (2014). Particulate matter and number concentrations of particles larger than 0.25 µm in the urban atmosphere of Jeddah, Saudi Arabia. *Aerosol Air Qual. Res.* 14: 1383–1391. https://doi.org/10.4209/aaqr.2014.02.0027

Hussein, T., Boor, B.E., dos Santos, V.N., Kangasluoma, J., Petäjä, T. and Lihavainen, H. (2017). Mobile aerosol measurement in the eastern Mediterranean – A Utilization of portable instruments. *Aerosol Air Qual. Res.* 17: 1875–1886. https://doi.org/10.4209/aaqr.2016.11.0479

Hussein, T., Juwhari, H., Al Kuisi, M., Alkattan, H., Lahlouh, B. and Al-Hunaiti, A. (2018). Accumulation and coarse mode aerosol concentrations and carbonaceous contents in the urban background atmosphere in Amman, Jordan. *Arab. J. Geosci.* 11: 617. https://doi.org/10.1007/s12517-018-3970-z

Hussein, T., Dada, L., Hakala, S., Petäjä, T. and Kulmala, M. (2019). Urban aerosol particle size characterization in eastern Mediterranean conditions. *Atmosphere* 10: 710. https://doi.org/10.3390/atmos10110710

Karanasiou, A., Moreno, N., Moreno, T., Viana, M., De Leeuw, F. and Querol, X. (2012). Health effects from Sahara dust episodes in Europe: Literature review and research gaps. *Environ. Int.* 47: 107–114. https://doi.org/10.1016/j.envint.2012.06.012

Kchih, H., Perrino, C. and Cherif, S. (2015). Investigation of desert dust contribution to source apportionment of PM_{10} and $PM_{2.5}$ from a southern Mediterranean coast. *Aerosol Air Qual. Res.* 15: 454–464. https://doi.org/10.4209/aaqr.2014.10.0255

Keramat, A., Marivani, B. and Samsami, M. (2011). Climatic change, drought and dust crisis in Iran. *WASET J.* 57: 10–13. https://doi.org/10.5281/zenodo.1058935

Khaniabadi, Y. O., Daryanoosh, S. M., Amrane, A., Polosa, R., Hopke, P. K., Goudarzi, G., Mohammadi, M. J., Sicard, P. and Armin, H. (2017). Impact of Middle Eastern Dust storms on human health. *Atmos. Pollut. Res.* 8: 606–613. https://doi.org/10.1016/j.apr.2016.11.005

Kok, J.F., Parteli, E.J., Michaels, T.I. and Karam, D.B. (2012). The physics of wind-blown sand and dust. *Rep. Prog. Phys.* 75: 106901. http://doi.org/10.1088/0034-4885/75/10/106901

Léon, J.F. and Legrand, M. (2003). Mineral dust sources in the surroundings of the north Indian Ocean. *Geophys. Res. Lett.* 30: 1309. https://doi.org/10.1029/2002GL016690

McTainsh, G. and Strong, C. (2007). The role of aeolian dust in ecosystems. *Geomorphology* 89: 39–54. https://doi.org/10.1016/j.geomorph.2006.07.028

Menéndez, I., Diaz-Hernandez, J.L., Mangas, J., Alonso, I. and Sánchez-Soto, P.J. (2007). Airborne dust accumulation and soil development in the North-East sector of Gran Canaria (Canary Islands, Spain). *J. Arid Environ.* 71: 57–81. https://doi.org/10.1016/j.jaridenv.2007.03.011

Middleton, N.J. (1986a). A geography of dust storms in South-west Asia. *Int. J. Climatol.* 6: 183–196. https://doi.org/10.1002/joc.3370060207

Middleton, N.J. (1986b). Dust storms in the Middle East. *J. Arid Environ.* 10: 83–96. https://doi.org/10.1016/S0140-1963(18)31249-7

Middleton, N.J. (2017). Desert dust hazards: A global review. *Aeolian Res.* 24: 53–63. https://doi.org/10.1016/j.aeolia.2016.12.001

Miller, R.L., Cakmur, R.V., Perlwitz, J., Geogdzhayev, I.V., Ginoux, P., Koch, D., Prigent, C., Ruedy, R., Schmidt, G.A. and Tegen, I. (2006). Mineral dust aerosols in the NASA Goddard Institute for Space Sciences ModelE atmospheric general circulation model. *J. Geophys. Res.* 111: D06208. https://doi.org/10.1029/2005JD005796

Munir, S., Habeebullah, T.M., Mohammed, A.M., Morsy, E.A., Rehan, M. and Ali, K. (2016). Analysing $PM_{2.5}$ and its association with PM_{10} and meteorology in the arid climate of Makkah, Saudi Arabia. *Aerosol Air Qual. Res.* 17: 453–464. https://doi.org/10.4209/aaqr.2016.03.0117

Nabavi, S.O., Haimberger, L. and Samimi, C. (2016). Climatology of dust distribution over West Asia from homogenized remote sensing data. *Aeolian Res.* 21: 93–107. https://doi.org/10.1016/j.aeolia.2016.04.002

Naimabadi, A., Ghadiri, A., Idani, E., Babaei, A.A., Alavi, N., Shirmardi, M., Khodadadi, A., Marzouni, M.B., Ankali, K.A., Rouhizadeh, A. and Goudarzi, G. (2016). Chemical composition of PM_{10} and its in vitro toxicological impacts on lung cells during the Middle Eastern Dust (MED) storms in Ahvaz, Iran. *Environ. Pollut.* 211: 316–324. https://doi.org/10.1016/j.envpol.2016.01.006

Natsagdorj, L., Jugder, D. and Chung, Y. S. (2003). Analysis of dust storms observed in Mongolia during 1937–1999. *Atmos. Environ.* 37: 1401–1411. https://doi.org/10.1016/S1352-2310(02)01023-3

Notaro, M., Yu, Y. and Kalashnikova, O.V. (2015). Regime shift in Arabian dust activity, triggered by persistent Fertile Crescent drought. *J. Geophys. Res.* 120: 10–229. https://doi.org/10.1002/2015JD023855

Pope III, C.A., Burnett, R.T., Thun, M.J., Calle, E.E., Krewski, D., Ito, K. and Thurston, G.D. (2002). Lung cancer, cardiopulmonary mortality, and long-term exposure to fine particulate air pollution. *JAMA* 287: 1132–1141. http://doi.org/10.1001/jama.287.9.1132

Pope III, C.A. and Dockery, D.W. (2006). Health effects of fine particulate air pollution: Lines that connect. *J. Air. Waste. Manage. Assoc.* 56: 709–742. https://doi.org/10.1080/10473289.2006.10464485

Prospero, J.M., Ginoux, P., Torres, O., Nicholson, S.E. and Gill, T.E. (2002). Environmental characterization of global sources of atmospheric soil dust identified with the Nimbus 7 Total Ozone Mapping Spectrometer (TOMS) absorbing aerosol product. *Rev. Geophys.* 40: 1002. https://doi.org/10.1029/2000RG000095

Querol, X., Alastuey, A., Rodrıguez, S., Viana, M.M., Artınano, B., Salvador, P., Mantilla, E., Garcia do Santos, S., Fernandez Patier, R., De La Rosa, J., Sanchez de la Campa, A., Menéndez, M. and Gil, J.J. (2004). Levels of particulate matter in rural, urban and industrial sites in Spain. *Sci. Total Environ.* 334: 359–376. https://doi.org/10.1016/j.scitotenv.2004.04.036

Querol, X., Tobías, A., Pérez, N., Karanasiou, A., Amato, F., Stafoggia, M., Pérez García-Pando, C., Ginoux, P., Forastiere, F., Gumy, S., Mudu, P. and Alastuey, A. (2019). Monitoring the impact of desert dust outbreaks for air quality for health studies. *Environ. Int.* 130: 104867. https://doi.org/10.1016/j.envint.2019.05.061

Rashki, A., Kaskaoutis, D.G., Francois, P., Kosmopoulos, P.G. and Legrand, M. (2015). Dust-storm dynamics over Sistan region, Iran: Seasonality, transport characteristics and affected areas. *Aeolian Res.* 16: 35–48. https://doi.org/10.1016/j.aeolia.2014.10.003

Rezazadeh, M., Irannejad, P. and Shao, Y. (2013). Climatology of the Middle East dust events. *Aeolian Res.* 10: 103–109. https://doi.org/10.1016/j.aeolia.2013.04.001

Saeifar, M.H. and Alijani, B. (2019). Detection of dust storm origins in the middle east by remotely sensed data. *J. Indian Soc. Remote Sens.* 47: 1883–1893. https://doi.org/10.1007/s12524-019-01030-5

Satheesh, S.K., Deepshikha, S. and Srinivasan, J. (2006). Impact of dust aerosols on Earth–atmosphere clear-sky albedo and its short wave radiative forcing over African and Arabian regions. *Int. J. Remote Sens.* 27: 1691–1706. https://doi.org/10.1080/01431160500462162

Shao, Y., Raupach, M.R. and Findlater, P.A. (1993). Effect of saltation bombardment on the entrainment of dust by wind. *J. Geophys. Res.* 98: 12719–12726. https://doi.org/10.1029/93JD00396

Singer, A., Ganor, E., Dultz, S. and Fischer, W. (2003). Dust deposition over the Dead Sea. *J. Arid Environ.* 53: 41–59. https://doi.org/10.1006/jare.2002.1023

Small, I., Van der Meer, J. and Upshur, R.E. (2001). Acting on an environmental health disaster: The case of the Aral Sea. *Environ. Health Perspect.* 109: 547–549. https://doi.org/10.1289/ehp.01109547

Solomos, S., Kalivitis, N., Mihalopoulos, N., Amiridis, V., Kouvarakis, G., Gkikas, A., Binietoglou, I., Tsekeri, A., Kazadzis, S., Kottas, M., Pradhan, Y., Proestakis, E., Nastos, P.T. and Marenco, F. (2018). From tropospheric folding to Khamsin and Foehn winds: How atmospheric dynamics advanced a record-breaking dust episode in Crete. *Atmosphere* 9: 240. https://doi.org/10.3390/atmos9070240

Stein, A.F., Draxler, R.R., Rolph, G.D., Stunder, B.J., Cohen, M.D. and Ngan, F. (2015). NOAA's HYSPLIT atmospheric transport and dispersion modeling system. *Bull. Am. Meteorol. Soc.* 96: 2059–2077. https://doi.org/10.1175/BAMS-D-14-00110.1

Taheri, A., Aliasghari, P. and Hosseini, V. (2019). Black carbon and $PM_{2.5}$ monitoring campaign on the roadside and residential urban background sites in the city of Tehran. *Atmos. Environ.* 218: 116928. https://doi.org/10.1016/j.atmosenv.2019.116928

Thomas, D.S., Knight, M. and Wiggs, G.F. (2005). Remobilization of southern African desert dune systems by twenty-first century global warming. *Nature* 435: 1218–1221. https://doi.org/10.1038/nature03717

Torres, O., Bhartia, P.K., Herman, J.R., Ahmad, Z. and Gleason, J. (1998). Derivation of aerosol properties from satellite measurements of backscattered ultraviolet radiation: Theoretical basis. *J. Geophys. Res.* 103: 17099–17110. https://doi.org/10.1029/98JD00900

World Health Organization (WHO) (2018). Global Ambient Air Quality Database (update 2018, accessed on March 20, 2020, https://www.who.int/airpollution/data/cities/en/). Ambient (outdoor) air quality database 2018 by country and city (https://www.who.int/airpollution/data/aap_air_uality_database_2018_v14.xlsx?ua=1,ap_air_quality_database_2018_v14.xlsx)

Zender, C.S., Bian, H. and Newman, D. (2003). Mineral Dust Entrainment and Deposition (DEAD) model: Description and 1990s dust climatology. *J. Geophys. Res.* 08: 4416. https://doi.org/10.1029/2002JD002775

Zoljoodi, M., Didevarasl, A. and Saadatabadi AR. (2013). Dust events in the western parts of Iran and the relationship with drought expansion over the dust-source areas in Iraq and Syria. *Atmos. Clim. Sci.* 3: 321–336. https://doi.org/10.4236/acs.2013.33034

Received for review, May 4, 2020
Revised, July 23, 2020
Accepted, September 14, 2020